



Ann Med Res

Current issue list available at [Ann Med Res](https://annalsmedres.org)

Annals of Medical Research

journal page: annalsmedres.org

Determination of density ranges to be used in grading hepatosteatosi s using computed tomography

Gulhan Kilcarslan

Elazığ Fethi Sekin City Hospital, Clinic of Radiology, Elazığ, Türkiye

*Corresponding author: dr.gulhankilcarslan@gmail.com (Gulhan Kilcarslan)

■ MAIN POINTS

- This retrospective study analyzed a cohort of 666 individuals to establish computed tomography (CT) density thresholds for quantifying hepatic steatosis.
- Patients were initially classified based on the grade of hepatosteatosi s determined by ultrasound.
- Subsequent CT density measurements of the liver were performed to define precise Hounsfield Unit (HU) ranges that can differentiate between these steatosis grades.
- A key anatomical finding was that Segment I (the caudate lobe) demonstrated the highest attenuation values, identifying it as the liver segment most resistant to fatty infiltration.

■ ABSTRACT

Aim: To determine the density ranges to evaluate the degree of hepatosteatosi s on computed tomography (CT) grades.**Materials and Methods:** Patients who were diagnosed with hepatosteatosi s by ultrasonography and those who subsequently underwent tomography were included in the study. Measurements were made from each segment of the liver and the spleen in the CT images of the graded groups. Liver/spleen density ratios were compared.**Results:** In total 666 patients were included for evaluation in the present study. Liver/spleen density ratios for Grade 1, Grade 2, and Grade 3 were 0.94 ± 0.19 , 0.70 ± 0.16 , and 0.37 ± 0.13 , respectively. There was a statistically significant difference in the Liver/spleen density ratios throughout all grades ($p=.001$). The cut-off value separating Grade 1 and Grade 2 was calculated as 0.77, and the cut-off value separating Grade 2 and Grade 3 was calculated as 0.47. Segment 1, which had the least fat accumulation, was significantly different from all the other segments.**Conclusion:** In the present study, it was determined that both contrast-enhanced and non-contrast-enhanced tomography can be used for the evaluation of hepatosteatosi s. However, contrast-enhanced tomography has been found to distinguish Grade 1 from Grade 2 more effectively than unenhanced CT.

Cite this article as: Kilcarslan G. Determination of density ranges to be used in grading hepatosteatosi s using computed tomography. *Ann Med Res.* 2025;32(9):394–400. doi: [10.5455/annalsmedres.2025.04.082](https://doi.org/10.5455/annalsmedres.2025.04.082).

Keywords: Hepatosteatosi s, Density range, Computed tomography, Ultrasonography**Received:** Apr 09, 2025 **Accepted:** Jul 21, 2025 **Available Online:** Sep 25, 2025

Copyright © 2025 The author(s) - Available online at annalsmedres.org. This is an Open Access article distributed under the terms of Creative Commons Attribution-NonCommercial-NoDerivatives 4.0 International License.

■ INTRODUCTION

Liver steatosis, or fatty liver, is the accumulation of triglycerides in hepatocytes over time [1-4]. Hepatosteatosi s is considered when 5% or more fat makes up its weight [5]. The prevalence is quite high, affecting more than 16-31% of the world's population [3,6-8]. Hepatosteatosi s is significant because it involves an inflammatory process that can lead to chronic liver disease [2,4,7,8]. It is often diagnosed incidentally during abdominal ultrasonography (US) examination [3].

Liver biopsy is considered the gold standard for diagnosing and classifying hepatosteatosi s [1,4,6,9,10]. However, it has several disadvantages, such as being an invasive procedure, the possibility of sampling error [1,4,6,10]. In cases of heterogeneous steatosis, a biopsy can yield misleading results [4]. For

these reasons, various imaging methods and laboratory parameters have been used to detect fat accumulation [4,9,10].

Ultrasonography is the most common diagnostic method because of its noninvasive nature, low cost, and absence of ionizing radiation [1,3,5,6,8,11]. The sensitivity for detecting steatosis ranges from 60-94%, and the specificity ranges from 84-95% [1,5]. Sensitivity increases when steatosis is moderate to severe [5,7]. However, the accuracy of diagnosis decreases in patients with low fat accumulation (below 20%) [1,3-6,8]. The main disadvantage of US is that it is dependent on the operator and the equipment used [1-4,7]. US can also be used to grade the extent of steatosis [4-6,8,11-13].

Grade 1 (G1) steatosis is defined as a slight increase in liver echogenicity compared with the adjacent renal parenchyma. The borders of the intrahepatic vessels remain sharp. Grade

2 (G2) steatosis is defined as a moderate increase in liver echogenicity, accompanied by a reduction in the echogenicity of the intrahepatic vascular structures and distortion of the diaphragm contour. Grade 3 (G3) steatosis is defined as a marked increase in liver echogenicity leads to blurring of the diaphragm contour, inability to distinguish the vessel walls, and difficulty in visualizing the posterior segments of the liver [4,6,8,11-13].

The clinical utility of this nonquantitative ultrasonographic assessment, which is based on operator-dependent echogenicity increases, is controversial [4,11]. Computed tomography reveals liver steatosis as a diffuse or heterogeneous decrease in parenchymal density [1,8,11]. Increased fat accumulation correlated with a greater decrease in density [1,3,4]. While the accuracy of CT in detecting liver steatosis varies, its sensitivity is reported to be 93%, with a positive predictive value of 76% [2,7]. Although CT is very sensitive in detecting moderate to severe steatosis, it is less effective for mild cases [7,11]. The use of non-contrast CT in clinical practice for detecting liver steatosis [1,4,7,10,11]. Some studies suggest that measurements taken during the portal venous phase in contrast-enhanced CT are more specific than those in non-contrast CT [14,15].

To assess liver steatosis, the liver parenchymal density, liver-spleen density difference (L-S), or liver-spleen density ratio (L/S) are measured [4,7,9,11]. The literature indicates that in healthy individuals, liver parenchymal density on non-contrast CT ranges from 45-65 hounsfield unit (HU), 50-57 HU, or 50-65 HU, with a liver density 8-10 HU higher than the spleen density [3,4,16]. A liver density less than 40 HU suggests presence of more than 30% steatosis [3,8]. One study defined a normal L-S range as 1-18 HU, where patients with a liver density of 48 HU and an L-S difference of -2 were identified as having moderate to severe steatosis [7]. Iwasaki et al. determined the L/S ratio in patients with no or mild steatosis to be approximately 1.184 ± 0.091 and set a threshold of 1.1 for distinguishing between mild and moderate to severe steatosis [9]. An L/S ratio less than 1 indicates hepatosteatosis [3]. Additionally, an L/S ratio less than 0.8 or an L-S difference greater than 9 HU indicates more than 30% hepatosteatosis [8].

Proton density fat fractionation MRI derivative (MRI-PDFF) has emerged as the most prevalent method for fat quantification in recent years, as it facilitates simultaneous whole organ imaging and organ tissue quantification. The MRI-PDFF technique facilitates the evaluation of individual hepatic segments [17,18]. The Quantitative Imaging Biomarkers Alliance (QIBA) MRI PDFF committee has presented data that confirms the accuracy of MRI in determining fat fraction over a wide range [19].

The objective of this study was to ascertain the HU ranges that facilitate grading by conducting density measurements on CT images of patients diagnosed with hepatosteatosis via US.

■ MATERIALS AND METHODS

This study was approved by the Ethics Committee of Firat University (date: 01.02.2024/ session number 02-37). Since the study was retrospective and no personal data were used, informed consent was not obtained. Patient lists were obtained by searching the term "hepatosteatosis" in US reports from our hospital database. To reduce operator variability, only patients reported by a single radiologist were evaluated. A total of 10,320 patients diagnosed with hepatosteatosis on USG were included for analysis. A total of 1,504 patients who underwent re-imaging were excluded from the study. The remaining patients were examined for the presence of CT images. CT imaging was available for 3,560 patients. Of these patients, 2011 underwent a CT scan in close temporal proximity to the US procedure (± 2 Weeks). Patients were excluded from the study if they did not undergo equilibrium phase imaging or if they underwent arterial phase imaging, in cases with a lesion in the liver, and if the imaging field did not include the entire liver or spleen. Patients suffering from chronic liver parenchymal disease and known alcohol abuse were also excluded from the study. The remaining 666 patients constituted the study cohort. Of these patients, 105 had contrast and non-contrast CT images obtained during the same period. The images of 105 patients with contrast and non-contrast imaging were dynamic images, and the non-contrast and equilibrium phases were used in the examination. The selected patients were classified according to the grades specified in their US reports.

The US assessments were conducted by a radiologist with 13 years of experience using a Philips Affiniti 50 device with a convex probe at 6-2 MHz. Liver echogenicity was graded based on the visibility of the vascular walls and diaphragm contours (Figure 1).

CT examinations were performed via a 128-slice CT scanner (Ingenuity Core 128; Philips Medical Systems, Best, Netherlands). Regions of interest (ROI) measuring 100-150 mm² were placed separately in the 8 segments of the liver. Three separate measurements were taken from the spleen parenchyma (Figure 2). The averages of these measurements were calculated, and the L/S ratios were determined. The HU values of each segment were also recorded. When placing the ROIs, care was taken to avoid artefacts, and blood vessels. In cases of heterogeneous density reductions, measurements were taken from more hypodense areas.

Since our measurements were taken from both contrast-enhanced and non-contrast images, we found that it was more appropriate to use the L/S ratio for evaluation. To compare the results of patients with both contrast-enhanced and non-contrast imaging, we performed calculations on both sets of images.

Statistical analysis

The data were analyzed via IBM SPSS 22.0 software (IBM SPSS Corp.; Armonk, NY, USA). The descriptive statistics of

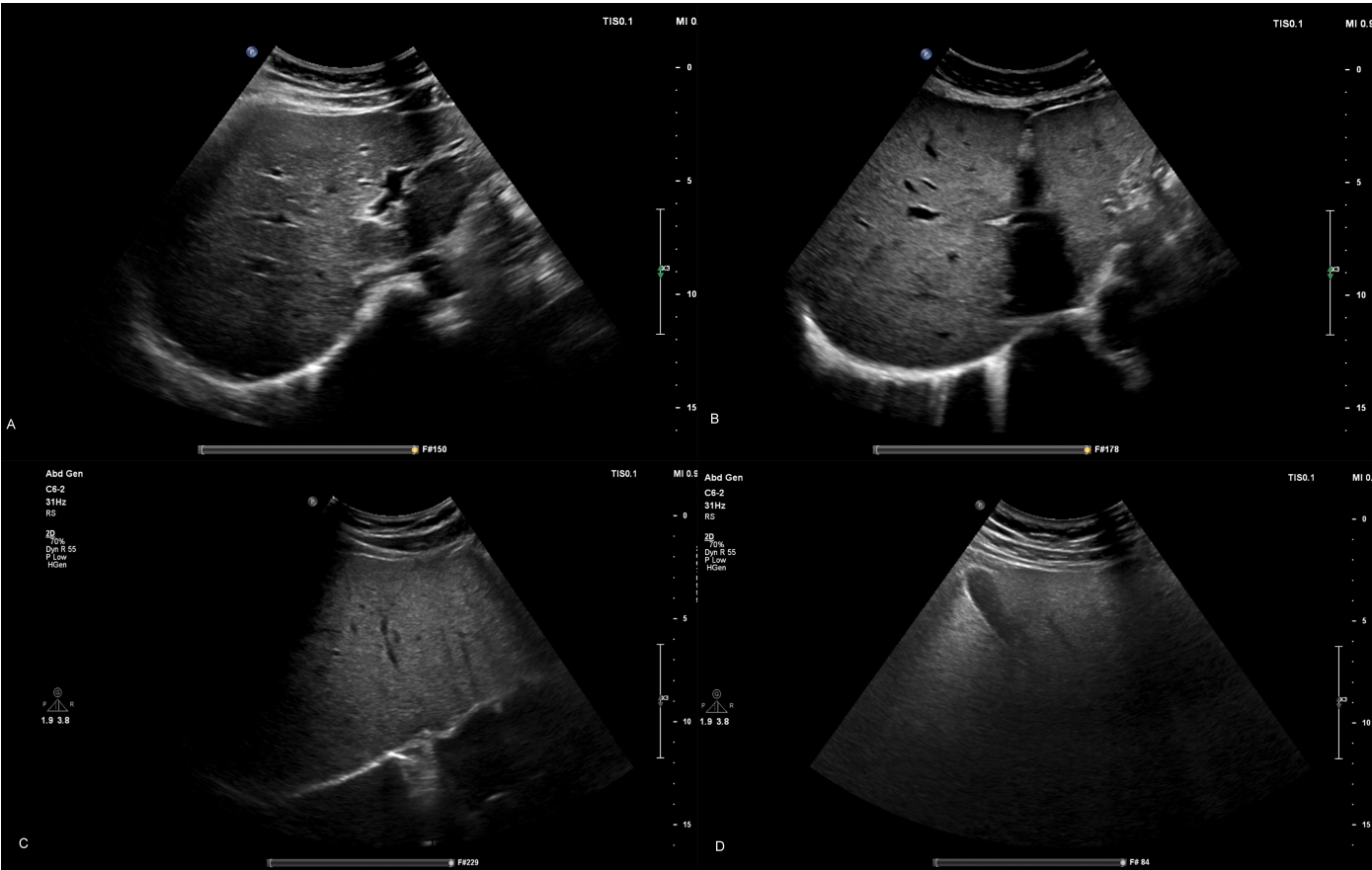


Figure 1. Liver US images according to grade. Grade 0 (A), Grade 1 (B), Grade 2 (C), Grade 3 (D).

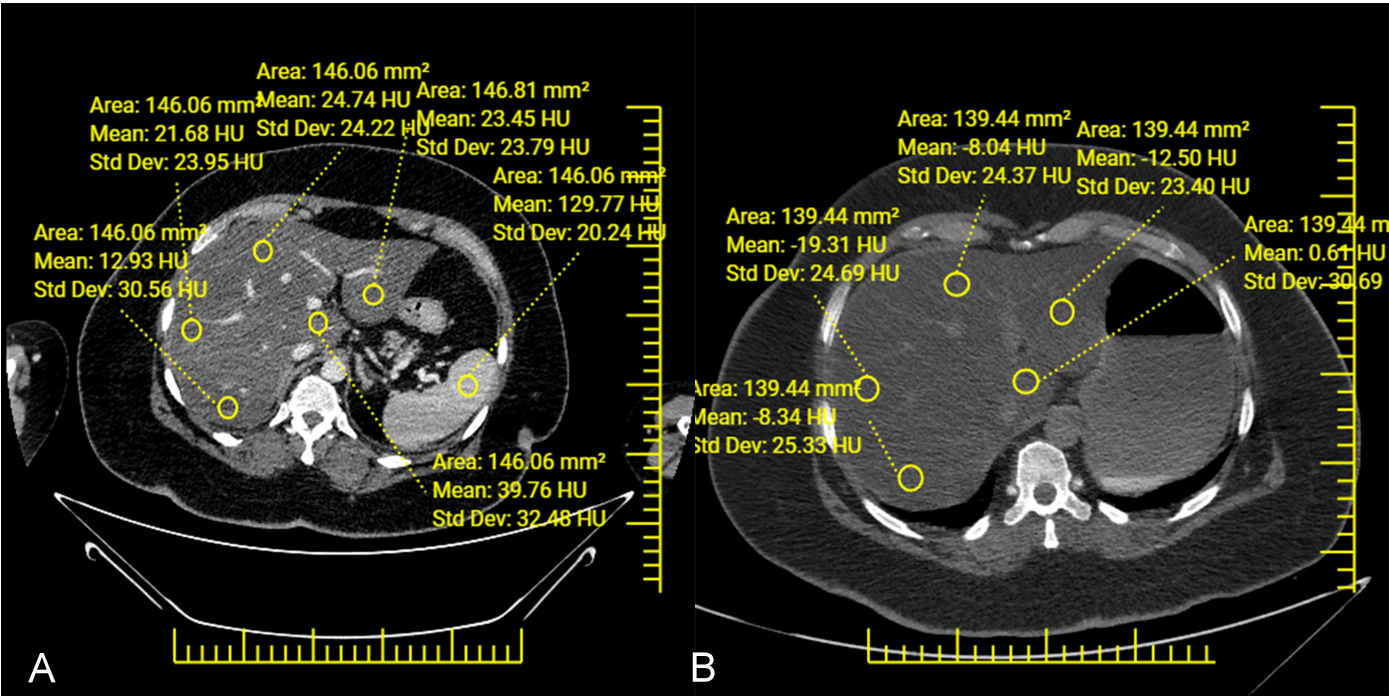


Figure 2. Placement of ROIs for computed tomography density measurement. (A) Axial CT image showing standard ROI placement in spleen and liver segments 1, 3, 4b, 5, and 6. (B) A supplemental image showing ROI placement in liver segments 1, 2, 4a, 8, and 7. ROIs were positioned to avoid visible vessels and bile ducts and to ensure representative sampling of parenchymal density.

the data are presented as the mean ± standard deviation, median (minimum–maximum), frequency, and percentage val-

ues. The normal distribution of variables was assessed via the Kolmogorov-Smirnov test. For the analysis of quantitative re-

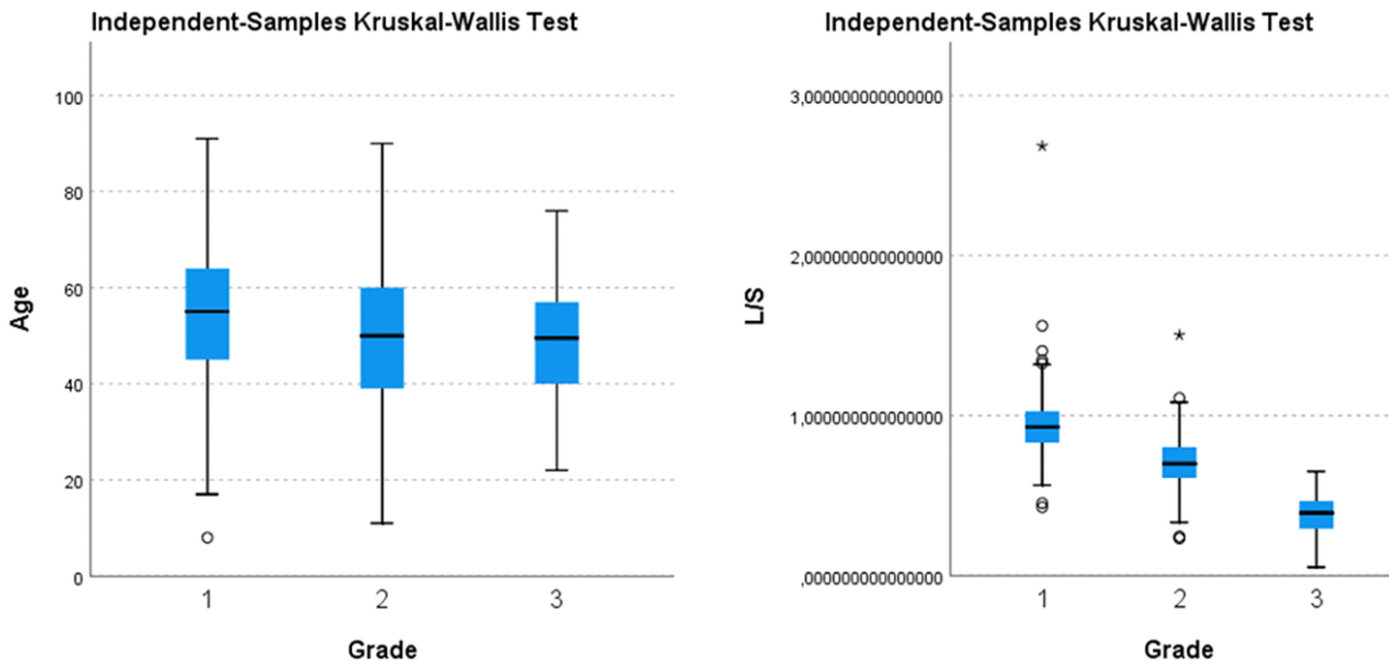


Figure 3. Comparison of age and L/S ratio of groups shown with a graph.

peated measures, the Friedman test was used, followed by the Dunn-Bonferroni correction as a post-hoc test. For the analysis of independent quantitative measurements, the Kruskal-Wallis test was used, followed by the Dunn-Bonferroni post-hoc correction. ROC analysis was used to determine the cutoff value, and the results are presented with the cutoff value calculated based on the area under the curve (AUC) and Youden index. A p value of 0.05 was considered statistically significant.

■ RESULTS

A total of 666 individuals, including 349 men and 317 women, met the inclusion criteria and were analyzed in the study. The characteristics of the patients, categorized by grade, are presented in Table 1. The average age of patients in G1 was significantly different from those in G2 and G3 ($p<.008$). The L/S ratios for G1, G2, and G3 were 0.94 ± 0.19 , 0.70 ± 0.16 , and 0.37 ± 0.13 , respectively. There was a statistically significant difference in the L/S ratios among all the groups ($p=.001$) (Figure 3). A ROC analysis was conducted to determine the threshold L/S values distinguishing the groups. For G1-G2, the area under the curve (AUC) was 0.857, with a sensitivity of 86%, specificity of 71%, and cutoff value of 0.77. For G2-G3, the AUC was 0.954, with a sensitivity of 94%, specificity of 82%, and cutoff value of 0.47 (Figure 4).

The HU values for all eight liver segments were recorded for each patient (Table 2). Segment 1 had the highest average value (66.72 HU), whereas segment 7 had the lowest (58.65 HU). Comparisons revealed no significant difference in HU values between segments 7-8 ($p<.068$), segments 5-6,

segments 4-3, segments 4-2, and segments 3-2 ($p=1$). Significant differences were observed in other comparisons ($p<.001$). Segment 1, which had the least fat accumulation, was significantly different from all the other segments.

Additionally, 105 patients with both contrast-enhanced and non-contrast abdominal CT scans taken within close time frames or on the same day were classified by grade. Measurements were taken from both types of CT scans to calculate L/S values. Statistical comparisons of contrast-enhanced and non-contrast CT data were made, and a ROC analysis was

Table 1. Characteristics of patients classified according to degree of hepatosteatosis.

	n
Total cases	666
Gender (male/female)	349/317
Age (mean)	51.62
Contrast CT/non-contrast CT	360/306
Grade 1	337
Gender (male/female)	164/173
Contrast CT/non-contrast CT	185/152
Grade 2	249
Gender (male/female)	134/115
Contrast CT/non-contrast CT	137/112
Grade 3	80
Gender (male/female)	51/29
Contrast CT/non-contrast CT	38/42
CT with and without contrast	105
Grade 1	48
Grade 2	47
Grade 3	10

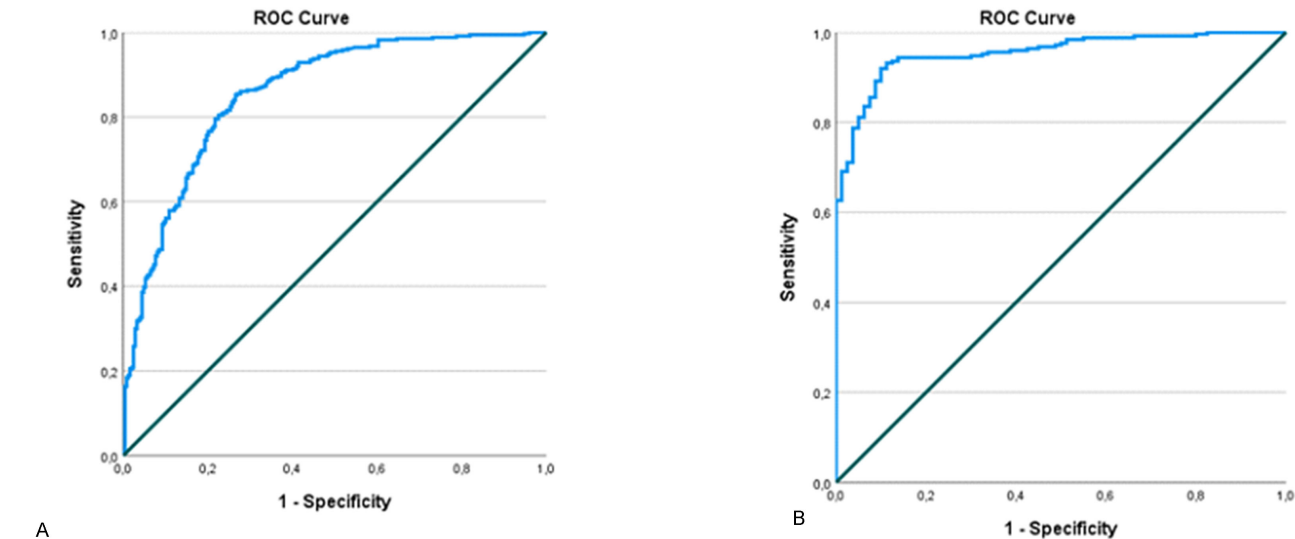


Figure 4. Determine the threshold L/S values separating the groups ROC analysis graphs. Area under the curve (AUC) for G1-G2 was 0.857 (A). AUC for G2-G3 was 0.954 (B).

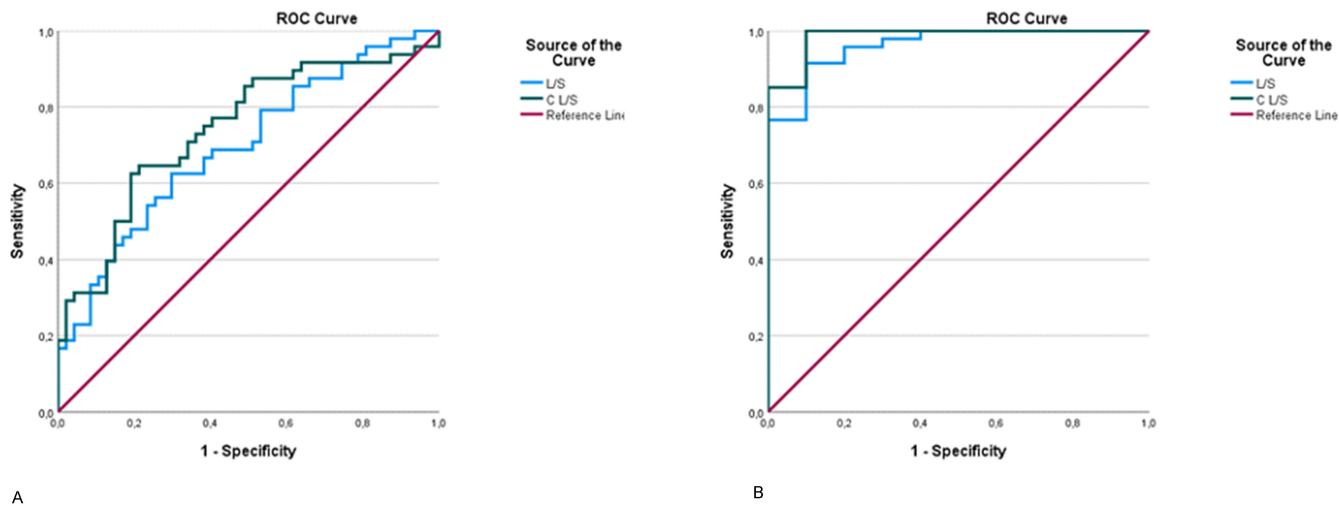


Figure 5. ROC analysis graphs of contrast and non-contrast CT data of the same patient. (A) For Grade 1-2, (B) For Grade 2-3. In both graphs, the AUC of contrast images is higher. L/S: Liver spleen HU ratio on noncontrast CT, CL/S: Liver spleen HU ratio on contrast enhanced CT.

Table 2. HU values of eight liver segments.

Liver segments	Minimum HU	Maximum HU	Mean HU	Std. Deviation
1	1	142	66.72	25.607
2	0	146	64.29	26.560
3	0	162	63.77	26.092
4	0	155	63.54	26.634
5	0	151	61.25	26.904
6	0	137	61.55	26.747
7	0	160	58.65	26.854
8	0	137	59.83	27.279

performed. The analysis of values from contrast-enhanced and non-contrast-enhanced imaging revealed significant dif-

ferences between the groups. However, contrast-enhanced images exhibited a higher degree of significance in distinguishing G1 and G2 (L/S p .003, L/S with contrast p .001). In the ROC analysis, the AUC for the G1-2 comparison was 0.695 for L/S and, 0.742 for L/S with contrast, indicating that contrast-enhanced imaging was more discriminative (Table 3, Figure 5). Segment 1 was found to be the least affected by fat accumulation. During the US evaluations, we observed focal, segmental, and lobar steatosis types. In the tomographic sections, lobar and segmental fatty deposits were observed in the G1 and G2 groups, while diffuse involvement was predominantly observed in the G3 group. It was also noteworthy that fatty deposits were more prevalent in the central parts.

Table 3. Comparison of measurements of patients who had CT scans with and without contrast.

	L/S			Contrast L/S		
	Mean HU	Min-Max HU	Std. Deviation	Mean HU	Min-Max HU	Std. Deviation
G1	0.98	0.57-1.32	0.168	0.86	0.42-2.68	0.300
G2	0.85	0.39-1.16	0.165	0.73	0.50-0.96	0.109
G3	0.31	0.02-0.73	0.252	0.40	0.23-0.62	0.112
	p			p		
G1-2	.003			.001		
G1-3	.001			.001		
G2-3	.001			.001		
	AUC	%95 Confidence Interval		AUC	%95 Confidence Interval	
G1-2	0.695	0.591	0.800	0.742	0.641	0.842
G2-3	0.962	0.910	1.000	0.985	0.954	1.000

■ DISCUSSION

Liver biopsy is the best diagnostic method for evaluating hepatosteatosis. However, for the diagnosis of simple hepatosteatosis, more non-invasive methods should be used instead of biopsy [6].

Hepatosteatosis is a condition that is common in all societies and is often detected incidentally with US. US, which has high sensitivity in detecting moderate and severe steatosis, has limited accuracy in detecting mild steatosis. Additionally, the detection of mild steatosis is variable because of user dependency. When there is less than 33% fat infiltration in the biopsy sample, the sensitivity of US decreases [7,13].

In daily practice, abdominal CT iamges are taken with contrast. Non-contrast CT is recommended especially for hepatosteatosis. Studies have shown that non-contrast and contrast-enhanced shots have similar accuracy rates [10].

In the study conducted by Kim et al. with 179 liver donors, contrast-enhanced CT was shown to be more successful than non-contrast CT [15].

In the study conducted by Johnston et al., contrast-enhanced CT detected hepatosteatosis with a sensitivity of 54-71% [10].

In this study, we performed measurements on existing CT images of patients with hepatosteatosis that we diagnosed and graded with US and determined the threshold HU value that separates the groups. We also performed measurements on contrast and non-contrast CT images of the same patient and examined which technique separated the groups better. Although there are many studies in literature, the measurements we made have not been made in any previous study.

Non-contrast CT is generally preferred because of contrast material delivery methods and scanning timing problems. We created our working groups by paying attention to this. Since we used images with and without contrast, it would not be correct to use only the liver HU value. Therefore, we used the liver HU/spleen HU value.

Although CT has high accuracy in the diagnosis of moderate and severe steatosis, it is not as sensitive in detecting mild

steatosis [3,7].

Iwasaki et al used various parameters to evaluate hepatosteatosis (L/S, BMI, GGTP, ALT, AST, Che, and T-CHO). These authors reported that the L/S ratio was strongly associated with steatosis. A single biopsy sample represents a very small part of the liver and cannot represent the entire liver. Therefore, CT allows the evaluation and measurement taken from every part of the liver [9].

In our study, we found a significant difference in the L/S values among the groups and calculated the threshold values that separate the grades. When comparing images with and without contrast, there was no significant difference in distinguishing G3 from G1 and G2, whereas CT with contrast was more significant in distinguishing G2 from G1. When the groups were compared, the area under the curve was greater in contrast-enhanced images. Some studies have shown that hepatosteatosis reduces hepatic blood flow [15]. This finding may explain why fatty segments are more hypodense during portal phase CT imaging. As a result, the increased fat lowers the average density of the liver and delays its contrast enhancement. In this case, we think that fatty segments become more prominent.

In addition, CT allowed us to measure each segment separately, and we found that segment 1 (Caudate lobe) had the least steatosis and that segment 7 had the highest. During the investigation, it was observed that the liver in patients G1 and G2 was partially fatty rather than diffusely. Liver biopsy is performed from the left lobe of the liver by a subcostal approach or from segments 5-6 by an intercostal approach. It is obvious that it is difficult to perform a biopsy from segment 7, where the most pronounced steatosis is seen. This finding suggests that not all biopsies will show the degree of hepatic steatosis with absolute certainty.

CT taken in the portal phase can detect hepatosteatosis with the same or even greater accuracy than non-contrast CT [15]. Several cross-sectional studies have reported heterogeneous steatosis among different lobes and segments. Research has been conducted on the alterations in fat distribution in-

sponse to weight gain and loss [17,20]. In the study conducted by Syvari et al. [17] with MRI-PDFF, mean liver and segmental steatosis values were calculated. Segment 1 had the least steatosis and segment 8 had the most. Segment 7 was the second most steatotic segment. Our study showed similar results with this study. In our study, the second most steatotic segment was 8 and the most diffusely steatotic segment was 7. We found very close results to MRI-PDFF measurements, which is reported to give the most accurate results for steatosis measurement in the literature. This also shows the accuracy of our US evaluation.

Limitations

The current study is not without limitations. Due to the retrospective nature of the study, it was not possible to obtain tissue diagnosis for the cases. There were limited number of G3 cases. Additionally, laboratory data from the imaging period were not available for each patient. It should be noted that weight and height data were not available for most patients.

CONCLUSION

As a result, hepatosteatois is a disease of increasing concern. US examinations are routinely used to determine the degree of fatty liver disease detected on CT images obtained for various reasons. MRI is not an easily accessible imaging modality. In this study, we determined grade-separating thresholds for grading hepatosteatois detected on CT without the need for USG or any other imaging technique. We believe that this approach will be useful for radiologists in grading and reporting hepatosteatois detected on CT and will eliminate the need for additional imaging.

Ethics Committee Approval: Ethical approval was obtained for the study from the Firat University Non-Interventional Research Ethics Committee (No: 2024/02-37). This retrospective study was conducted in accordance with the ethical standards of the institutional and/or national research committee and with the 1964 Helsinki Declaration and its later amendments or comparable ethical standards.

Informed Consent: Not necessary for this manuscript.

Peer-review: Externally peer-reviewed.

Conflict of Interest: The authors declare that they have no known competing financial interests or personal relationships that could have appeared to influence the work reported in this paper.

Financial Disclosure: This research did not receive any specific grant from funding agencies in the public, commercial, or not-for-profit sectors.

REFERENCES

1. Cerit M, Şendur HN, Cindil E, et al. Quantification of liver fat content with ultrasonographic attenuation measurement function: Correlation with unenhanced multidimensional computerized tomography. *Clin Imaging*. 2020;65: 85-93. doi: [10.1016/j.clinimag.2020.04.028](https://doi.org/10.1016/j.clinimag.2020.04.028).
2. Duman DG, Celikel C, Tüney D, Imeryüz N, Avsar E, Tözün N. Computed tomography in nonalcoholic fatty liver disease: a useful tool for hepatosteatois assessment? *Dig Dis Sci*. 2006;51(2): 346-51. doi: [10.1007/s10620-006-3136-9](https://doi.org/10.1007/s10620-006-3136-9).
3. Lăpădat AM, Jianu IR, Ungureanu BS, et al. Non-invasive imaging techniques in assessing non-alcoholic fatty liver disease: a current status of available methods. *J Med Life*. 2017;10(1): 19-26. PMID: [28255371](https://pubmed.ncbi.nlm.nih.gov/28255371/).
4. İdilman İS, Karçaaltınca M. Karaciğer Yağlanması Tanısında ve Yağlanma Miktarının Belirlenmesinde Radyolojik Tanı Yöntemleri. *Güncel Gastroenteroloji*. 2014;18(1):112-118.
5. Toprak D. Hepatosteatois (Fatty Liver Disease). *The Journal of Turkish Family Physician*. 2011;2(2):50-7.
6. Lee SJ, Kim YR, Lee YH, Yoon KH. US Attenuation Imaging for the Evaluation and Diagnosis of Fatty Liver Disease. *J Korean Soc Radiol*. 2023;84(3):666-75. doi: [10.3348/jksr.2022.0053](https://doi.org/10.3348/jksr.2022.0053).
7. Lee SS, Park SH. Radiologic evaluation of nonalcoholic fatty liver disease. *World J Gastroenterol*. 2014; 20(23):7392-402. doi: [10.3748/wjg.v20.i23.7392](https://doi.org/10.3748/wjg.v20.i23.7392).
8. Alkol Dışı Yağlı Karaciğer Hastalığı (NAFLD) Klinik Rehberi. Yılmaz Y (editor). Ankara: *Türk Karaciğer Araştırmaları Derneği*. 2021; p. 3-32.
9. Iwasaki M, Takada Y, Hayashi M, et al. Noninvasive evaluation of graft steatosis in living donor liver transplantation. *Transplantation*. 2004;78(10):1501-5. doi: [10.1097/01.tp.0000140499.23683.0d](https://doi.org/10.1097/01.tp.0000140499.23683.0d).
10. Aktas E, Uzman M, Yildirim O, et al. Assessment of hepatic steatosis on contrast enhanced computed tomography in patients with colorectal cancer. *Int J Clin Exp Med*. 2014;7(11):4342-6. PMID: [25550952](https://pubmed.ncbi.nlm.nih.gov/25550952/).
11. Gürses B, Seçil M. Diffüz Karaciğer Hastalıkları. *Türk Radiol Semin*. 2015;3(3):349-65. doi: [10.5152/trs.2015.286](https://doi.org/10.5152/trs.2015.286).
12. Saadeh S, Younossi ZM, Remer EM, et al. The utility of radiological imaging in nonalcoholic fatty liver disease. *Gastroenterology*. 2002;123(3):745-50. doi: [10.1053/gast.2002.35354](https://doi.org/10.1053/gast.2002.35354).
13. Yılmaz A, Yılmaz F, Beydilli İ, et al. Ultrasonographically detected hepatosteatois independently predicts the presence and severity of coronary artery disease. *Afr Health Sci*. 2022;22(2):273-85. doi: [10.4314/ahs.v22i2.31](https://doi.org/10.4314/ahs.v22i2.31).
14. Lawrence DA, Oliva IB, Israel GM. Detection of hepatic steatosis on contrast-enhanced CT images: diagnostic accuracy of identification of areas of presumed focal fatty sparing. *AJR Am J Roentgenol*. 2012;199(1):44-7. doi: [10.2214/AJR.11.7838](https://doi.org/10.2214/AJR.11.7838).
15. Kim DY, Park SH, Lee SS, et al. Contrast-enhanced computed tomography for the diagnosis of fatty liver: prospective study with same-day biopsy used as the reference standard. *Eur Radiol*. 2010;20(2):359-66. doi: [10.1007/s00330-009-1560-x](https://doi.org/10.1007/s00330-009-1560-x).
16. Karaarslan GT. Canlı vericili karaciğer nakillerinde donörlerde pre-transplant dönemde çok dedektörlü bilgisayarlı tomografi (ÇDBT) ile hesaplanan greft volümünün cerrahi sonrası greft ağırlığı ile karşılaştırılması ve bulguların analizi. *İstanbul Bilim Üniversitesi*; 2012.
17. Syväri J, Junker D, Patzelt L, et al. Longitudinal changes on liver proton density fat fraction differ between liver segments. *Quant Imaging Med Surg*. 2021;11(5):1701-1709. doi: [10.21037/qims-20-873](https://doi.org/10.21037/qims-20-873).
18. Yoshizawa E, Yamada A. MRI-derived proton density fat fraction. *J Med Ultrason (2001)*. 2021;48(4):497-506. doi: [10.1007/s10396-021-01135-w](https://doi.org/10.1007/s10396-021-01135-w).
19. Dyke JP. Quantitative MRI Proton Density Fat Fraction: A Coming of Age. *Radiology*. 2021;298(3):652-653. doi: [10.1148/radiol.2020204356](https://doi.org/10.1148/radiol.2020204356).
20. Fazeli Dehkordy S, Fowler KJ, Mamidipalli A, et al. Hepatic steatosis and reduction in steatosis following bariatric weight loss surgery differs between segments and lobes. *Eur Radiol*. 2019;29(5):2474-2480. doi: [10.1007/s00330-018-5894-0](https://doi.org/10.1007/s00330-018-5894-0).